THE JOURNAL OF BIOLOGICAL CHEMISTRY VOL. 287, NO. 6, pp. 4129–4138, February 3, 2012
Published in the U.S.A.

Analysis of the Mobilities of Band 3 Populations Associated with Ankyrin Protein and Junctional Complexes in Intact Murine Erythrocytes*[S]

Received for publication, August 16, 2011, and in revised form, November 30, 2011 Published, JBC Papers in Press, December 6, 2011, DOI 10.1074/jbc.M111.294439

Gayani C. Kodippili[‡], Jeff Spector[§¶], Jacob Hale[§], Katie Giger[‡], Michael R. Hughes[‖], Kelly M. McNagny[‖], Connie Birkenmeier[**], Luanne Peters[**], Ken Ritchie[§1], and Philip S. Low[‡2]

*From the [‡]Department of Chemistry, Purdue University, West Lafayette, Indiana 47907, the [§]Department of Physics, Purdue University, West Lafayette, Indiana 47907, the [¶]National Institute of Standards and Technology, Gaithersburg, Maryland 20899, the [‖]Biomedical Research Centre, University of British Columbia, Vancouver, British Columbia V6T 1Z3, Canada, and the **Jackson Laboratory, Bar Harbor, Maine 04609*

Background: Erythrocyte band 3 exists in three populations; ankyrin-bound, adducin-bound, and free.
Results: In wild-type murine erythrocytes, ~40% of band 3 is attached to ankyrin, ~33% is immobilized by adducin, and ~27% is free.
Conclusion: Ankyrin- and adducin-bound band 3 can be monitored separately.
Significance: This diffusion study demonstrates molecular differences between band 3 complexes and reveals structural heterogeneity within band 3 subpopulations.

Current models of the erythrocyte membrane depict three populations of band 3: (i) a population tethered to spectrin via ankyrin, (ii) a fraction attached to the spectrin-actin junctional complex via adducin, and (iii) a freely diffusing population. Because many studies of band 3 diffusion also distinguish three populations of the polypeptide, it has been speculated that the three populations envisioned in membrane models correspond to the three fractions observed in diffusion analyses. To test this hypothesis, we characterized band 3 diffusion by single-particle tracking in wild-type and ankyrin- and adducin-deficient erythrocytes. We report that ~40% of total band 3 in wild-type murine erythrocytes is attached to ankyrin, whereas ~33% is immobilized by adducin, and ~27% is not attached to any cytoskeletal anchor. More detailed analyses reveal that mobilities of individual ankyrin- and adducin-tethered band 3 molecules are heterogeneous, varying by nearly 2 orders of magnitude and that there is considerable overlap in diffusion coefficients for adducin and ankyrin-tethered populations. Taken together, the data suggest that although the ankyrin- and adducin-immobilized band 3 can be monitored separately, significant heterogeneity still exists within each population, suggesting that structural and compositional properties likely vary considerably within each band 3 complex.

Early models of the human erythrocyte membrane contained little structural detail, displaying primarily a phospholipid bilayer juxtaposed to a contiguous spectrin-based cortical cytoskeleton, with minimal information on the physical linkages connecting the two adjacent layers (1, 2). Because lipid bilayers were already known to be intrinsically unstable (3, 4), research rapidly focused on identifying linkages between the fragile bilayer and the more stable spectrin-based membrane skeleton that might stabilize the bilayer. A protein complex composed of the membrane-spanning protein, band 3 (AE1), linked to spectrin via ankyrin, was the first bridge shown to perform this linking function (5–10). Evidence for the critical role of the band 3-ankyrin bridge came not only from studies of membranes in which the bridge was artificially ruptured (11–13) and from characterization of band 3-knock-out mice (14, 15), but also from observations that natural mutations in any of the bridging components commonly led to an inherited membrane instability termed hereditary spherocytosis (16–19). More recent studies then revealed that additional bridges between the lipid bilayer and the spectrin-based membrane skeleton might similarly contribute to membrane stability, including bridges between band 3 and adducin (20), glycophorin C (21), and protein 4.1 (22, 23) and GLUT1 (24) and dematin (2, 25–27). Perhaps most prominent among these latter bridges was the linkage between band 3 and adducin at the spectrin-actin junctional complex because dissociation of this bridge was shown to cause membrane fragmentation (20).

Based on these and other considerations, three populations of band 3 are now believed to exist in the erythrocyte membrane: (i) an ankyrin-attached population located near the center of the spectrin tetramer, (ii) an adducin-linked population situated at the spectrin-actin junctional complex, and (iii) an unattached population that should be free to diffuse laterally unless transiently obstructed by other membrane or cytoskeletal proteins (Fig. 1). Unfortunately, the many independent analyses of band 3 diffusion in erythrocyte membranes do not agree on the number of distinct band 3 species in the mem-

* This work was supported, in whole or in part, by National Institute of Health Grant GM24417-32 (to P. S. L.). This work was also supported by National Science Foundation Grant 0646633 (to K. R.) and Canadian Institutes for Health Research Grant MOP-93580 (to K. M. M.).
[S] This article contains supplemental Figs. 1 and 2 and supplemental text.
[1] To whom correspondence may be addressed: Dept. of Physics, Purdue University, 525 Northwest Ave., West Lafayette, IN 47909. E-mail: kpritchie@purdue.edu.
[2] To whom correspondence may be addressed: Dept. of Chemistry, Purdue University, 560 Oval Dr., West Lafayette, IN 47907. E-mail: plow@purdue.edu.

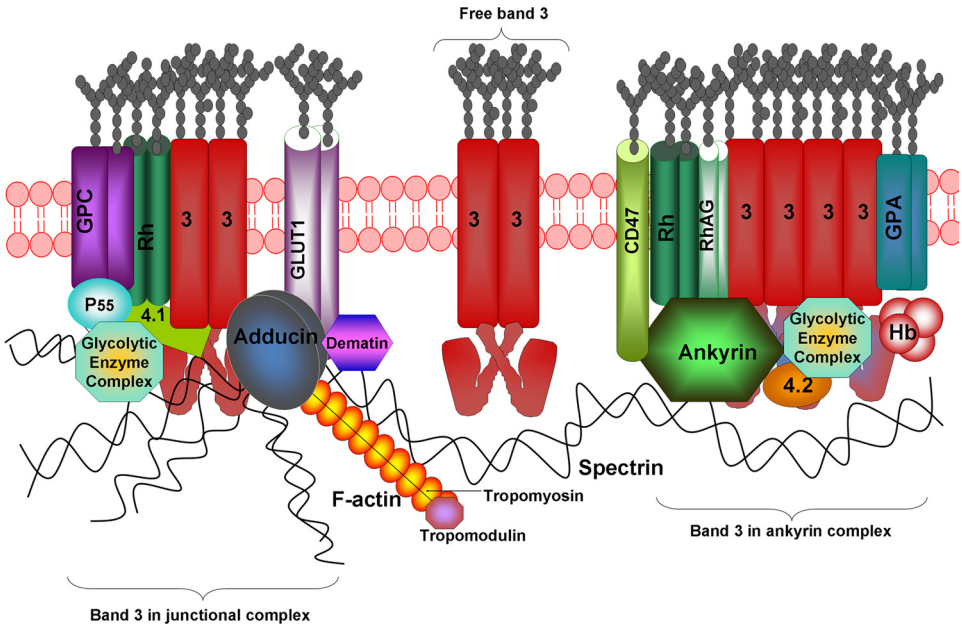

FIGURE 1. **Organization of major membrane protein complexes in human erythrocyte membrane.** *GLUT1*, glucose transporter 1; *3*, band 3 or AE1; *GPA*, glycophorin A; *GPC*, glycophorin C; *Hb*, hemoglobin; *4.1*, protein 4.1; *4.2*, protein 4.2; *RhAG*, Rh-associated glycoprotein.

brane. Whereas early studies of band 3 rotational diffusion suggested two rotating populations (28, 29), more recent analyses using more advanced techniques suggest three rotating populations (30–32). Moreover, fluorescence recovery after photobleaching (30, 33, 34) and single-particle tracking experiments (35–37) from multiple laboratories generally detect only two fractions of the anion transporter *in situ*. A recent paper from the Golan laboratory (38), however, observes three populations of band 3. The question thus arises whether two or three populations of band 3 actually exist in healthy erythrocytes and if three exist, whether they correlate directly with the three fractions defined in the recent biochemical studies (30–32).

To begin to characterize the different populations of band 3 in intact erythrocytes, we have labeled single molecules of band 3 in fresh murine erythrocytes with 4,4′-diisothiocyano-2,2′-stilbenedisulfonic acid (DIDS)[3]-tethered quantum dots and have recorded their diffusion trajectories in intact cells using high speed videomicroscopy (35). Evaluation of these single-particle tracking experiments at 120 frames/s (fps) reveals three distinct populations of band 3 in healthy murine red cells. The purpose of this publication is to report our analysis of band 3 diffusion in erythrocytes from mice with mutations in the two bridges that tether the anion transporter to the spectrin/actin cytoskeleton. Our data suggest that adducin- and ankyrin-tethered populations of band 3 display overlapping mobilities and that independent characterization of these two populations can be achieved by examination of ankyrin- or adducin-deficient erythrocytes.

EXPERIMENTAL PROCEDURES

Mice Blood-collecting Protocol—Blood samples were obtained from normal mice and mice with deficiencies in ankyrin (nb/nb) (39) and adducin (β-adducin-null (40) and α-adducin-null (41, 42)) maintained at The Jackson Laboratories. E924X (13) (nearly quantitative ankyrin deficiency) mouse blood was obtained from mice maintained at The Biomedical Research Centre, University of British Columbia, Vancouver, BC, Canada. Blood was collected into heparin tubes (Sigma H-3393) and labeled with DIDS-biotin conjugate, as described previously (40, 41, 43) and further elaborated in the supplemental text.

Single-quantum Dot Fluorescence Video Microscopy—Labeling of approximately one band 3 molecule/erythrocyte with a quantum dot using a DIDS-biotin conjugate was performed as described previously (35) and as outlined in greater detail in the supplemental text. However, because band 3 diffuses differently in erythroblasts and reticulocytes than it does in mature red cells (44), it was important to exclude any cells containing RNA from our measurements of band 3 diffusion, especially in blood samples from ankyrin- or adducin-deficient erythrocytes where reticulocyte counts are high. For this purpose, analysis of band 3 diffusion in mutant erythrocytes (supplemental Fig. 1) was only performed on cells that were labeled with a quantum dot but not with SYTO RNASelect. The 488-nm emission line of an argon ion laser (Newport) was used to excite the SYTO RNASelect stain, whereas the 543 nm emission line of a helium-neon laser (Newport) was used to excite the quantum dots. Both excitation lines were expanded, filtered (488/10-nm and 543/10-nm line width bandpass filters, respectively; Chroma) and directed toward the microscope objective (100× PlanApo, NA 1.45 TIRFM oil immersion; Olympus) parallel, but off the optical axis through a dual dichroic mirror (double notch filter centered at the excitation lines, z488/543rpc; Chroma). Oblique angle illumination was obtained by slightly relaxing the condition of total internal reflection such that only a part of the sample chamber was illuminated while still minimizing the background. After passing through the dual dichroic mirror, the two-color fluorescent image was split by wavelength using a

[3] The abbreviations used are: DIDS, 4,4′-diisothiocyano-2,2′-stilbenedisulfonic acid; D_M, macroscopic diffusion coefficient; D_μ, microscopic diffusion coefficient; fps, frames per second; nb, normoblastosis.

high pass cutoff filter (545 nm; Chroma). The separated emission lines were filtered by broad band transmission filters (515/30 nm, Chroma; and 630/69 nm, Semrock) before being collected by two dual MCP-intensified, cooled CCD cameras (XR/Turbo-120z, Stanford Photonics). A sample of 20-nm fluorescent polystyrene beads fixed to a coverslip was used to align the two camera images. Micrometer screws along five axes (*x*, *y*, *z*, tilt and twist) on one camera were used to match its field of view with that of the other camera. The entire microscope was maintained at 37 °C by enclosure in a temperature-controlled environment.

Analysis of Mobility—The apparent position of the quantum dot in the video image was determined as described by Gelles *et al.* (45). Briefly, a two-dimensional kernel was developed from a Gaussian distribution which was then cross-correlated with each video frame in the neighborhood of the label of interest. Details of analyses have been explained previously (35). A plug-in was written for the freely available ImageJ software which allowed analysis of the single-particle diffusion trajectories. Data obtained at 120 frames per second (fps) were processed to yield 30 fps data (by averaging the raw 120 fps data every 4 frames) and found to yield diffusion parameters identical to data collected directly at 30 fps. Statistical analyses are described in supplemental text.

RESULTS

Labeling of Band 3—Characterization of the movement of single band 3 molecules in whole erythrocytes required the ability to specifically label band 3, the erythrocyte anion transporter (AE1), in intact cells in a nonperturbing manner. For this purpose, DIDS, a selective inhibitor of anion transport that reacts covalently with Lys^{539} of band 3 (46), was conjugated to biotin and employed to label a single band 3 molecule in intact cells. The specificity of the DIDS-biotin conjugate for mouse band 3 was established by reacting the conjugate with intact mouse erythrocytes, separating the component proteins by SDS-PAGE, blotting the proteins onto nitrocellulose paper, and visualizing the location of biotinylated polypeptides by staining with streptavidin-horseradish peroxidase. As seen in supplemental Fig. 2, only one polypeptide with apparent molecular mass of ~100 kDa was labeled. Because band 3 is the only known erythrocyte receptor for DIDS and because band 3 has the molecular mass of the protein stained in supplemental Fig. 2 (*i.e.* ~100 kDa), we conclude that band 3 is selectively labeled by the DIDS-biotin conjugate in intact murine erythrocytes. The fact that streptavidin-linked quantum dots do not bind erythrocytes that have not been reacted with DIDS-biotin (35) demonstrates that DIDS-biotin labeling enables selective imaging of band 3 diffusion in intact murine erythrocytes. Because only enough DIDS-biotin is added to label one band 3 molecule per erythrocyte and because diffusion measurements are obtained <1 h after labeling, we do not believe that the labeling reaction measurably affects erythrocyte properties.

Analysis of Band 3 Mobility at Different Frame Rates—Before describing the rates of band 3 diffusion in healthy murine erythrocytes, a brief explanation of the effect of videomicroscopy frame rate on the calculation of band 3 diffusion coefficients might be helpful. Imagine three populations of band 3: one oscillating in a confined area at high frequency; a second oscillating in a slightly larger area at somewhat slower frequency; and a third diffusing in an unconstrained and random manner across large regions of the membrane. A few photographs of the position of band 3 at long time intervals would likely reveal that the first two populations were confined to a limited area, whereas the third diffused randomly across the cell. In contrast, the same number of photographs taken at extremely short time intervals would reveal that the first two populations were moving rapidly, perhaps even at sufficiently different rates to distinguish them from each other, with the third population, although highly mobile, moving only a short distance. Thus, to obtain a complete understanding of the different motile populations of band 3, data must be analyzed at different frame rates for different durations, and their different areas of confined diffusion must be considered. We have used this more detailed multiframe rate approach to study band 3 diffusion in wild-type and mutant mouse erythrocytes.

Characterization of the Microscopic Diffusion Coefficients (D_μ) of Band 3 in Normal and Ankyrin-deficient Murine Erythrocytes—The microscopic diffusion coefficient (D_μ) reports on particle diffusion over short time periods and thereby emphasizes its instantaneous motility rather than sustained motility. A typical distribution of D_μ values of band 3 in normal murine RBCs collected at 120 fps is shown in Fig. 2, *row A*, *column 1* (see Table 1). With the aid of computer analysis (see "Experimental Procedures"), three populations of band 3 can be identified and fit to Gaussian distributions, one diffusing at 6.3×10^{-12} cm^2/s (~22% of total), a second diffusing at 6.3×10^{-11} cm^2/s (~66% of total), and a third population diffusing at 8.3×10^{-10} cm^2/s (~12% of total). Although it was tempting to assume that the three different populations correspond to adducin-linked band 3 at the junctional complex, ankyrin-attached band 3 midway along the spectrin tetramer, and free band 3 not attached to the spectrin cytoskeleton, respectively, we sought to test these assumptions by analyzing band 3 diffusion in erythrocytes from mice with deficiencies in adducin and ankyrin. As seen in Fig. 2, *row B*, *column 1*, E924X mice that are nearly completely deficient in ankyrin display two broad (probably heterogeneous) distributions of band 3 species, one with microscopic diffusion coefficients (D_μ) centered at 1.1×10^{-10} cm^2/s (~60% of total) and the second with D_μ centered at 2.1×10^{-9} cm^2/s (~40% of total). Although it was not possible to establish which band 3 population(s) was diffusing more rapidly in the ankyrin-deficient RBCs (despite analysis of >500 ankyrin-deficient erythrocytes), it was clear that the fraction of band 3 diffusing at ~10^{-9} cm^2/s increases upon loss of ankyrin from ~12% to ~40% of the total band 3.

To exploit the unique information available from analyses of single-molecule diffusion at different frame rates, the microscopic diffusion of band 3 in wild-type and E924X erythrocytes was next examined at 30 fps. As seen in *row A*, *column 3*, only one prominent population of band 3 is resolved in healthy erythrocytes at this slower frame rate, displaying a mean D_μ of 6.6×10^{-12} cm^2/s and comprising ~95% of the band 3. Importantly, in ankyrin-deficient mice (*row B*, *column 3*) (Table 1), this single Gaussian distribution segregates into three distinct populations of band 3 with D_μ values of 1.3×10^{-12} cm^2/s (17%

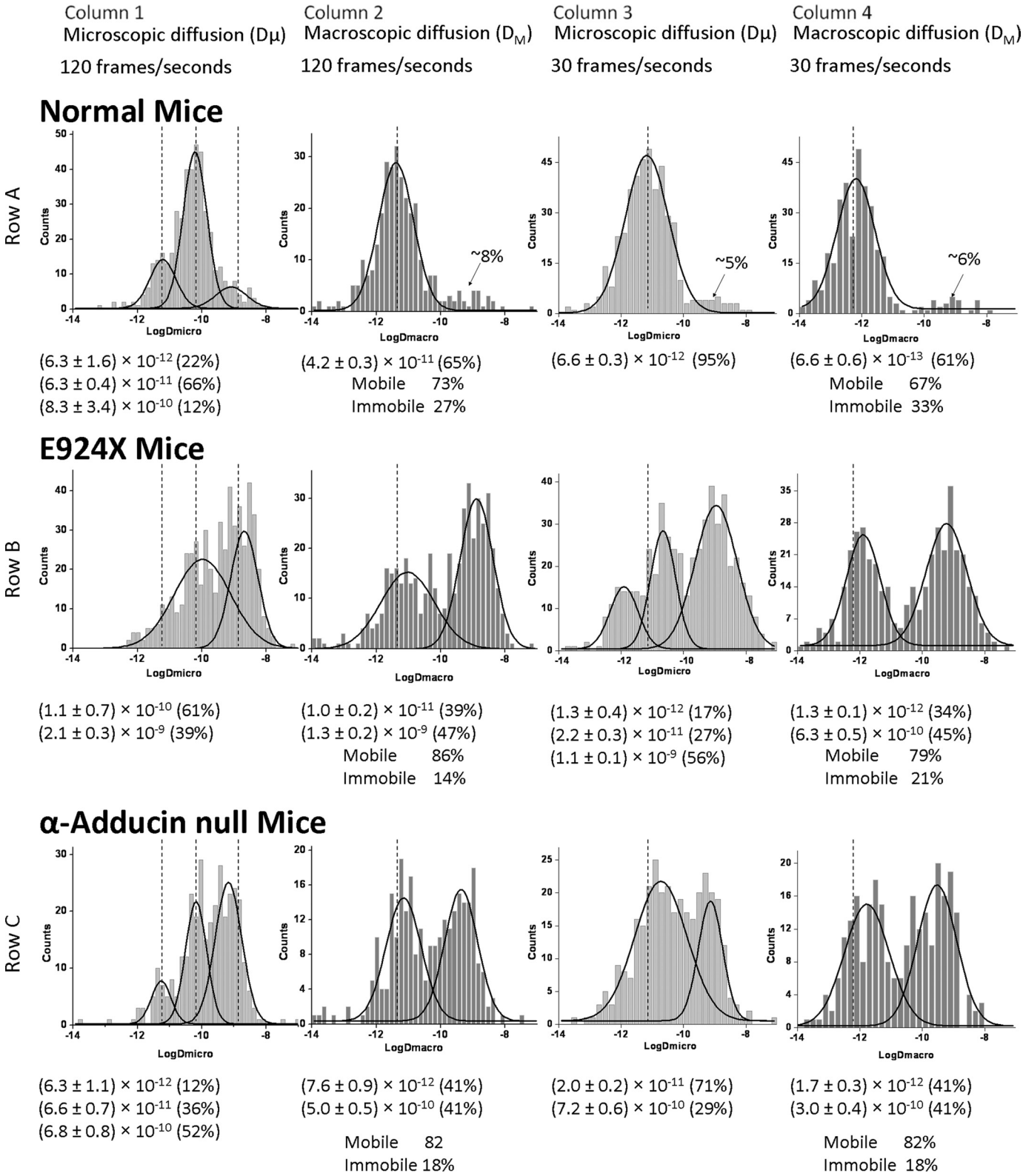

FIGURE 2. **Histogram plots of diffusion coefficients of labeled band 3 molecules in intact normal, ankyrin-null (E924X), and α-adducin-null erythrocyte membranes.** Distributions of the logarithms of D_μ and D_M were determined by analysis of individual trajectories of labeled band 3 molecules on intact normal, α-adducin-null, and ankyrin-null (E924X) erythrocytes at 120 fps (bin size of 0.15 on histograms) and 30 fps (bin size of 0.2 on histograms) (see "Experimental Procedures"). For comparison purposes, the *dotted line* shows the position of the middle of the distribution of each major Gaussian curve present in wild-type erythrocytes measured under the same conditions. Below each *panel*, the mean diffusion coefficient of each population is provided, along with the percent of the total band 3 present in that population. Although all molecules of band 3 appear mobile over short time spans (D_μ), a measurable fraction appears to be immobilized over long time spans (D_M). This fraction is also listed below each histogram of D_M values. The sizes of the adducin- and ankyrin-linked populations were calculated by subtracting the minor population of rapidly diffusing band 3 in normal erythrocytes (denoted with an *arrow* and quantitated as a percentage of total band 3; see *row A*) from the same fraction of rapidly diffusing band 3 in each mutant cell type.

TABLE 1
Microscopic and macroscopic diffusion data of normal and mutant mouse RBCs at 120 and 30 fps

RBC type	D_μ at 120 fps	D_M at 120 fps	Immobile fraction	D_μ at 30 fps	D_M at 30 fps	Immobile fraction
	cm^2/s	cm^2/s	%	cm^2/s	cm^2/s	%
Fixed ($n = 134$)	$(6.8 \pm 0.1^a) \times 10^{-14}$	$(5.5 \pm 0.2) \times 10^{-14}$	95[b]	$(1.5 \pm 0.1) \times 10^{-13}$	$(1.3 \pm 0.2) \times 10^{-14}$	95[b]
Normal ($n = 541$)[c]	$(6.3 \pm 1.6) \times 10^{-12}$ (22%) $(6.3 \pm 0.4) \times 10^{-11}$ (66%) $(8.3 \pm 3.4) \times 10^{-10}$ (12%)	$(4.2 \pm 0.3) \times 10^{-11}$ (65%)	27	$(6.6 \pm 0.3) \times 10^{-12}$ (95%)	$(6.6 \pm 0.6) \times 10^{-13}$ (61%)	33
E924X ($n = 554$)	$(1.1 \pm 0.7) \times 10^{-10}$ (61%) $(2.1 \pm 0.3) \times 10^{-9}$ (39%)	$(1.0 \pm 0.2) \times 10^{-11}$ (39%) $(1.3 \pm 0.2) \times 10^{-9}$ (47%)	14	$(1.3 \pm 0.4) \times 10^{-12}$ (17%) $(2.2 \pm 0.3) \times 10^{-11}$ (27%) $(1.1 \pm 0.1) \times 10^{-9}$ (56%)	$(1.3 \pm 0.1) \times 10^{-12}$ (34%) $(6.3 \pm 0.5) \times 10^{-10}$ (45%)	21
nb/nb ($n = 294$)	$(5.9 \pm 0.8) \times 10^{-11}$ (100%)	$(6.0 \pm 0.5) \times 10^{-12}$ (62%) $(1.0 \pm 0.2) \times 10^{-9}$ (17%)	21	$(1.2 \pm 0.1) \times 10^{-11}$ (83%) $(1.2 \pm 0.5) \times 10^{-9}$ (17%)	$(1.2 \pm 0.1) \times 10^{-12}$ (59%) $(4.6 \pm 0.8) \times 10^{-10}$ (12%)	29
α-Adducin-null ($n = 346$)	$(6.3 \pm 1.1) \times 10^{-12}$ (12%) $(6.6 \pm 0.7) \times 10^{-11}$ (36%) $(6.8 \pm 0.8) \times 10^{-10}$ (52%)	$(7.6 \pm 0.9) \times 10^{-12}$ (41%) $(5.0 \pm 0.5) \times 10^{-10}$ (41%)	18	$(2.0 \pm 0.2) \times 10^{-11}$ (71%) $(7.2 \pm 0.6) \times 10^{-10}$ (29%)	$(1.7 \pm 0.3) \times 10^{-12}$ (41%) $(3.0 \pm 0.4) \times 10^{-10}$ (41%)	19
β-Adducin-null ($n = 129$)	$(7.9 \pm 1.1) \times 10^{-11}$ (100%)	$(6.4 \pm 0.5) \times 10^{-12}$ (74%)	26	$(1.0 \pm 0.2) \times 10^{-11}$ (100%)	$(1.4 \pm 0.2) \times 10^{-12}$ (69%)	31

[a] Errors are given as the S.E.
[b] The totally immobile fraction is defined as the fraction of band 3 molecules that were found to have a D_M value ≤ the slowest 95% of D_M values measured for band 3 on fixed erythrocytes.
[c] Total number of trajectories analyzed.

of total), 2.2×10^{-11} cm^2/s (27% of total), and 1.1×10^{-9} cm^2/s (56% of total), with the last population being largely absent in the healthy erythrocytes. The appearance of this last population with a diffusion coefficient approximately 2 orders of magnitude faster than any band 3 seen in wild-type murine erythrocytes suggests that the absence of ankyrin enables roughly half of the band 3 to diffuse at a rate expected of unanchored band 3, *i.e.* $\sim 10^{-9}$ cm^2/s as reported by Golan and colleagues (47).

Characterization of Macroscopic Diffusion Coefficients (D_M) of Band 3 in Normal and Ankyrin-deficient Murine Erythrocytes—To explore the impact of ankyrin deficiency on band 3 mobility even further, we examined the diffusion of band 3 over long time periods, termed macroscopic diffusion coefficients (D_M), in both normal and ankyrin-deficient (E924X) murine red cells. Importantly, because D_M data are collected over much longer time periods, analyses of D_M data allow identification of a relatively stationary (termed immobile below) population of band 3 that cannot be easily resolved in D_μ analyses. As seen in Fig. 2, *row A*, *column 2* (Table 1), D_M measured at 120 fps is 4.2×10^{-11} cm^2/s in healthy cells (with 27% of the band 3 molecules being stationary or immobile on this time scale). Importantly, collection and analysis of the same data on ankyrin-deficient erythrocytes yield two distinct mobile populations characterized by D_M values of 1.0×10^{-11} cm^2/s (39% of total) and 1.3×10^{-9} cm^2/s (47% of total). The stationary or immobile fraction of band 3 in these analyses comprises 14% of the total. The fact that ~47% of the total band 3 diffuses ~100 times faster over these long time periods in the ankyrin-deficient erythrocytes confirms the earlier suggestion that roughly half of erythrocyte band 3 is ankyrin-linked in healthy mice.

Analysis of macroscopic diffusion coefficients of band 3 at 30 fps in normal and ankyrin-deficient erythrocytes yields a very similar result. As seen in Fig. 2, *row A*, *column 4* (Table 1), the distribution of D_M values measured at 30 fps in healthy cells is best fit by a single Gaussian comprising 61% of the cells with a mean value of 6.6×10^{-13} cm^2/s, and with ~33% being immobile. In contrast, D_M analyses under identical conditions in ankyrin-deficient cells yields two populations of band 3 with D_M values of 1.3×10^{-12} cm^2/s (34% of total) and 6.3×10^{-10} cm^2/s (45% of total), with 21% remaining immobile (Fig. 2, *row B*, *column 4*). The appearance of this new population comprising ~45% of the total band 3 that migrates ~2 orders of magnitude faster than band 3 in wild-type cells supports the contention that roughly half of the band 3 is released when the ankyrin tethers are absent.

Characterization of D_μ of Band 3 in Normal and Adducin-deficient Murine Erythrocytes—The α,β-adducin heterodimer has been shown to tether band 3 to spectrin at the junctional complex of the red cell membrane; *i.e.* where multiple spectrins associate in radial geometry with a central actin/protein 4.1/adducin hub. Importantly, whereas β-adducin-knock-out mice compensate for their deficiency in the β-subunit by up-regulating expression of the γ-adducin gene, α-adducin-null mice display nearly quantitative absence of all adducin isoforms, rendering the mouse essentially adducin-deficient (41). As seen in Fig. 2, *row C*, *column 1* (Table 1), D_μ values for band 3 in α-adducin-knock-out cells (hereafter termed adducin-deficient) change little from wild-type cells when the data are collected at 120 fps. Importantly, however, the relative sizes of the band 3 populations shift significantly. Thus, the band 3 population diffusing at $\sim 6.3 \times 10^{-12}$ cm^2/s in normal cells decreases from ~22% to 12% of the total in adducin-deficient cells. Similarly, the abundance of the band 3 population diffusing at $\sim 6 \times 10^{-11}$ cm^2/s decreases from ~66% to 36% of the total when adducin is absent. Finally, the fraction of the anion transporter diffusing at $\sim 8.3 \times 10^{-10}$ cm^2/s increases from ~12% to 52% of the total in the adducin-deficient cells. These data suggest that the adducin-linked fraction of band 3 may comprise up to ~40% of the total band 3 (*i.e.* freely diffusing band 3 increases from ~12 to ~52% of the total). More importantly, because both of the two slower populations decrease in abundance when the linkage to adducin is broken, the data further suggest that adducin-tethered band 3 in normal erythrocytes oscillates or diffuses at two distinct rates characterized by slow and intermediate D_μ values. Whether the residual band 3 that diffuses at these two slower rates is solely due to the ankyrin-linked population, (8, 9, 34) or alternatively, derives from an ankyrin-linked population plus another unidentified population of band 3 cannot be discerned from these data.

Analysis of D_μ values of band 3 in adducin-deficient erythrocytes at 30 fps suggests that ~30% of the band 3 diffuses more rapidly when adducin is absent (compare *column 3* in *rows A* and *C*). Thus, the single Gaussian distribution of D_μ values seen in healthy cells ($D_\mu = 6.6 \times 10^{-12}$ cm^2/s) separates into two populations with D_μ values of $\sim 2 \times 10^{-11}$ cm^2/s (~71% of total) and $\sim 7.2 \times 10^{-10}$ cm^2/s (29%) in adducin-deficient cells.

Characterization of D_M of Band 3 in Adducin-deficient Murine Erythrocytes—Analysis of the D_M of band 3 in adducin-deficient mice yields data that are consistent with the above data on D_μ (Table 1). Thus, at 120 fps, the single Gaussian distribution of D_M values segregates into two Gaussian distributions of $\sim 7.6 \times 10^{-12}$ cm^2/s (41% of the total) and $\sim 5.0 \times 10^{-10}$ cm^2/s (41%), with 18% appearing immobilized over these long time spans. Similarly, the single Gaussian seen at 30 fps divides into two populations with D_M values of $\sim 1.7 \times 10^{-12}$ cm^2/s (41%) and $\sim 3.0 \times 10^{-10}$ cm^2/s (41%), with 18% appearing immobile. Thus, at both 120 and 30 fps, ~41% of the band 3 diffuses ~2 orders of magnitude faster when adducin is missing from the cell. These data suggest that ~40% of the band 3 population is attached to the junctional complex via adducin.

Characterization of D_μ and D_M of Band 3 in Murine Erythrocytes That Are Only Partially Depleted of Either Ankyrin or Adducing—Whereas the E924X and α-adducin-knock-out mice are almost completely ankyrin- and adducin-deficient, respectively, two other commonly available mouse strains are only partially depleted of these two bridging proteins. Thus, nb/nb (39) mice express <5% of the normal amount of wild-type ankyrin, but this loss is partially compensated for by the production of a mutant ankyrin that lacks a regulatory domain, but retains the band 3 and spectrin binding domains (48). Red cells from nb/nb mice retain relatively normal looking architecture by electron microscopy with an ankyrin immunoreactive protein detected in the normal position in their red cell membranes (49). This suggests that the mutant ankyrin is incorporated into the membrane, but the linkage is less stable due to the lack of a functional regulatory domain. This could explain why band 3 diffusion in the mature nb/nb erythrocytes (reticulocytes eliminated) is only moderately abnormal (Fig. 3, Table 1). Although the tripartite distribution of D_μ values at 120 fps in normal cells was found to collapse into a single Gaussian distribution by the Origin program, the mean D_μ value in the nb/nb cells (Fig. 3, *row B*, *column 1*) remains similar to its value in wild-type mice (Fig. 3, *row A*, *column 1*). Except for the appearance of a fast diffusing population comprising ~20% of the total band 3 in the D_M data at 120 fps and in both D_μ and D_M data at 30 fps, no other prominent changes in band 3 mobility were discerned. These results suggest that a partial deficiency of ankyrin in nb/nb mice leads only to a moderate change in diffusion coefficients, where D_μ and D_M values reside somewhere between the corresponding parameters for wild-type cells and E924X cells.

Similar to the situation with the ankyrin hypomorph, the β-adducin-knock-out mice (40) largely compensate for their absence of β-adducin by up-regulating γ-adducin, which forms a native heterodimer with α-adducin and largely compensates for the β-adducin deficiency (41). Not surprisingly, the diffusion characteristics of band 3 in β-adducin-knock-out mice appear essentially normal at all frame rates and all lengths of data acquisition tested (Fig. 3 and Table 1).

Analysis of Compartment Sizes in Which Band 3 Is Free to Diffuse—In addition to calculation of D_μ and D_M values, videos of the band 3 trajectories can be analyzed for the compartment sizes in which band 3 diffusion appears to be confined. Fig. 4 shows the distribution of these compartment sizes in wild-type and the various mutated erythrocytes. In healthy murine red cells, ~95% of the band 3 is confined to diffuse within a range of compartments of <100-nm diameter. In contrast, in E924X erythrocytes, only 55% of the band 3 is confined in its movement to such small compartments. Intermediate between wild-type and E924X erythrocytes are nb/nb, α-adducin-null, and β-adducin-null red cells with 78%, 77%, and 94% of their band 3 molecules constrained to move within corrals of <100-nm diameter. At the opposite end of this compartment size spectrum are compartments of >400-nm diameter. The fraction of band 3 that is free to diffuse within compartments of this large dimension is 1%, 10%, 24%, 0%, and 5% for wild-type, nb/nb, E924X, β-adducin-null, and α-adducin-null red cells, respectively. Clearly, compartment size analyses correlate with diffusion rate measurements in revealing that the greatest freedom of band 3 mobility occurs in ankyrin- and adducin-null phenotypes compared with the less severe partial depletion mutants.

DISCUSSION

With the recent discovery of a population of erythrocyte membrane band 3 that is linked to adducin at the junctional complex (20), the question naturally arose regarding what proportion of anion transporters might be tethered to ankyrin and what fraction might be attached to adducin. Using the above single-particle tracking data, the sizes of these two populations can now be estimated by determining the fraction of band 3 that shifts from a slowly diffusing population to the most rapidly diffusing population upon deletion of either ankyrin or adducin. In the case of ankyrin deletion (E924X mice), the size of the most rapidly diffusing population assayed at 120 fps ($D_\mu \sim 10^{-9}$ cm^2/s) increases from 12% of the total in wild-type cells to 39% in ankyrin-deficient cells (Fig. 2, *column 1*, *rows A* and *B*), suggesting that 27% of band 3 might be immobilized by ankyrin. Comparison of D_M values between wild-type and ankyrin-deficient mice at the same frame rate reveals an increase in the most rapidly diffusing population of ~39% upon loss of ankyrin (Fig. 2, *column 2*, *rows A* and *B*, and Table 1). At 30 fps, the band 3 population with a D_μ of $\sim 10^{-9}$ cm^2/s increases by ~51% in the E924X mice relative to wild-type mice, and the same comparison for D_M values shows a rise of ~39% in the freely diffusing population (Fig. 2, *columns 3* and *4*, *rows A* and *B*). Taken together, an average of 39% of the band 3 in the murine erythrocyte membrane increases in mobility when ankyrin is missing from the cell. Based on these data, we propose that roughly 40% of band 3 must be ankyrin tethered in healthy erythrocytes (Fig. 2).

The validity of the aforementioned estimate of the number of ankyrin-linked band 3 molecules can now be tested for consistency with existing data, albeit from studies of human erythrocytes. Assuming there are ~1,200,000 molecules of band 3 and

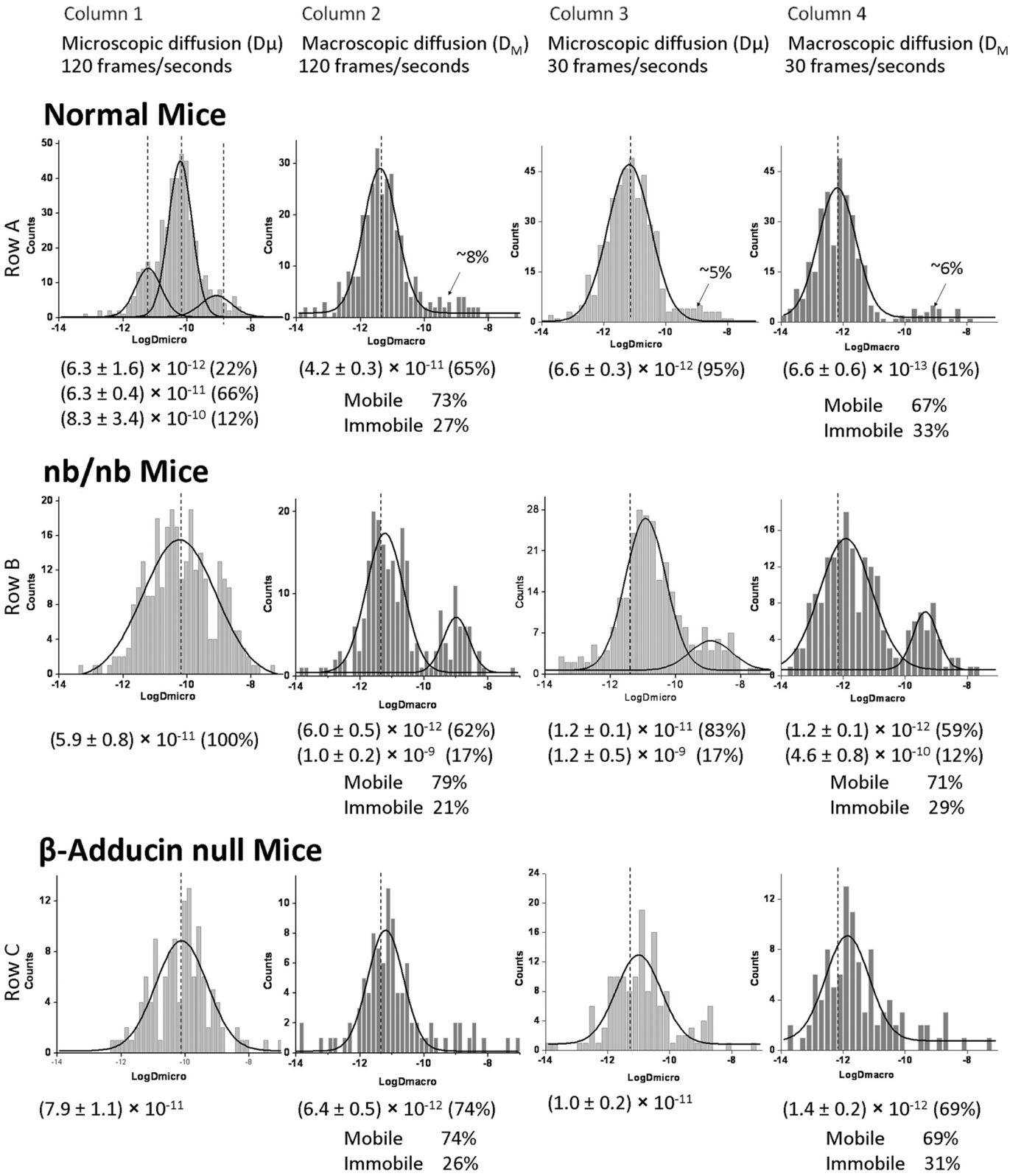

FIGURE 3. **Histogram plots of diffusion coefficients of labeled band 3 molecules in intact normal, partially ankyrin-deficient (nb/nb), and slightly adducin-deficient (*β*-adducin-null) erythrocyte membranes.** All other details are similar to those provided in the legend to Fig. 2.

~120,000 molecules of ankyrin per erythrocyte (50) and assuming that every ankyrin binds one tetramer of band 3 (8, 9), one can calculate that 40% (*i.e.* 480,000 molecules) of band 3 should be attached to ankyrin in a healthy erythrocyte. This agreement between theoretical prediction and experimental data suggests that single-particle tracking can provide quantitative information on the mobilities and related physical attributes of different subpopulations of band 3.

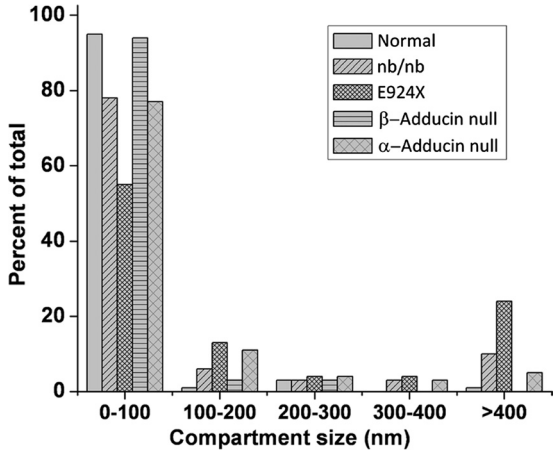

FIGURE 4. **Evaluation of band 3 compartment size from wild-type and mutant murine erythrocytes.** Distribution of the compartment sizes determined by analysis of individual trajectories of labeled band 3 molecules in intact normal murine, E924X (ankyrin-deficient), nb/nb (partially ankyrin-deficient), α-adducin-null, and β-adducin-null (mildly adducin-deficient) erythrocytes at 30 fps. Data present only the distribution of band 3 compartment sizes in mature RBCs.

A similar series of calculations can also be performed to estimate the fraction of band 3 that is tethered to adducin. Based on comparison of the percent band 3 in the highly mobile fraction of control and adducin-deficient erythrocytes, the sizes of the adducin-attached populations can be estimated to comprise 40%, 33%, 24%, and 35% of the total band 3 (calculated from the differences in D_μ and D_M values at both 120 and 30 fps between wild-type and adducin-deficient cells, respectively). The average of these independent estimates, *i.e.* ~33%, would suggest that roughly one-third of erythrocyte band 3 might be anchored to adducin at the spectrin-actin junctional complex (Fig. 2).

Independent confirmation of this latter estimate by numerical analysis is unfortunately more difficult, largely because much less information is available on the band 3-adducin complex. Although it is generally assumed that there are ~40,000 junctional complexes per cell (21, 24) and that each junctional complex requires one α,β-adducin heterodimer to cap the barbed end of the actin protofilament (51), there is no information regarding the band 3 oligomer state that binds adducin. However, because both α- and β-adducin subunits exhibit nanomolar affinity for band 3 (20), one can anticipate that each adducin heterodimer will bind two band 3 oligomers, enabling up to ~80,000 band 3 dimers or tetramers to be anchored at the junctional complex. If one assumes that the adducin-associated band 3 oligomer is a tetramer, then ~320,000 band 3 monomers or 27% of the total band 3 would be anchored to the junctional complex. Although this number is in reasonable agreement with our experimental data, it is also conceivable that not all adducin monomers will bind band 3 or that the interacting band 3 species will be dimeric rather than tetrameric. If either of these alternatives was to prove valid, the above estimate of adducin-linked band 3 would be too high and an alternative explanation for the magnitude of band 3 molecules immobilized by adducin would be required.

Because ankyrin- and adducin-deficient erythrocytes are only available in the mouse, a similar examination of band 3 population sizes in the human has not been possible. Nevertheless, the motile properties of band 3 in healthy murine and human erythrocytes can be compared to determine whether the mouse erythrocyte constitutes a good model for analysis of human band 3 diffusion. Because published data on normal murine (49, 52–55) and human (28–33, 37, 38, 56) erythrocytes have been collected under different measurement conditions (*i.e.* frame rate, O-step, bin size, etc.), it became necessary to repeat the single-particle tracking studies under identical conditions. Using a frame rate of 30 fps, an O-step of 10 and bin size of 0.2, D_μ and D_M values were found to be nearly identical for both species (data not shown). Moreover, at 120 fps, D_M values were again almost identical in the mouse and in the human. In contrast, at 120 fps, D_μ values segregated naturally into three populations in the mouse (Fig. 2) but resolved into only two populations in the human (33). Although this latter discrepancy suggests that protein interactions involving band 3 differ somewhat between mouse and human erythrocytes, we suspect that these differences may be minor because the prominent slowly diffusing population of band 3 in human erythrocytes displays an unusually broad distribution of D_μ values that has been previously interpreted to correspond to overlapping distributions of ankyrin- and adducin-attached band 3 (35). Assuming that the two slower diffusing populations in the mouse also correspond to ankyrin- and adducin-linked band 3, the behaviors of the two membranes would appear to be at least qualitatively comparable. Former and future studies of band 3 diffusion at different temperatures may provide further information on the similarities and differences between these two membrane systems (29, 47, 57).

When the distribution of D_μ values for band 3 in wild-type erythrocytes was first determined, it was tempting to speculate that the three Gaussian distributions seen in Fig. 2 (*row A*, *column 1*) would correspond to the three anticipated populations of band 3; *i.e.* adducin-attached, ankyrin-attached, and unattached band 3. The data obtained in this study, however, suggest that this interpretation may be oversimplified. For example, ankyrin-deficient red cells in the E924X mice yielded a D_μ profile at 30 fps that still contains three populations of band 3 (Fig. 2, *row B*, *column 3*, and Table 1). If only adducin-attached and free band 3 were still present in these ankyrin-deficient cells, only two Gaussian curves would have been anticipated. Therefore, unless an unidentified population of band 3 remains to be discovered, considerable heterogeneity must exist in either the adducin-linked or unattached populations to account for the above observations. Moreover, based on the data presented in Fig. 2 (*row C*, *column 1*, and Table 1), a related argument can be offered for the existence of heterogeneity within the ankyrin-attached fraction of band 3. These conclusions suggest that highly uniform models of red cell membrane architecture may be oversimplified and that heterogeneity in structure (and by inference composition) of individual junctional or ankyrin complexes likely exists. Indeed, although computer-generated fits of the diffusion data to overlapping Gaussian curves suggest distinct populations of band 3, examination of the widths at half-height of the individual Gaussians reveals a range of diffusion coefficients that spans up to 2 orders of magnitude. This extraordinary range of diffusion coefficients within a single Gaussian distribution also argues that constraints on

the mobilities of individual band 3 complexes are heterogeneous, even within a presumed single population of band 3. Some of this heterogeneity could arise from variabilities in the proximity of spectrin tetramers to the lipid bilayer or factors affecting spectrin self-association or flexibility. Alternatively, recognizing that band 3 (2), protein 4.2 (58), calmodulin, protein 4.1 (21, 59), spectrin, ankyrin, adducin (25), and many erythrocyte kinases (60) and phosphatases (61) are all known to have multiple binding partners with associations often regulated by biological stimuli, the above heterogeneity could have arisen from variabilities in the composition of band 3 complexes. Evaluation of additional mutants or earlier stages of erythroid differentiation should help clarify the fundamental causes of the above range of band 3 mobilities.

REFERENCES

1. Bruce, L. J., Ghosh, S., King, M. J., Layton, D. M., Mawby, W. J., Stewart, G. W., Oldenborg, P. A., Delaunay, J., and Tanner, M. J. (2002) Absence of CD47 in protein 4.2-deficient hereditary spherocytosis in man: an interaction between the Rh complex and the band 3 complex. *Blood* **100,** 1878–1885
2. Bruce, L. J., Beckmann, R., Ribeiro, M. L., Peters, L. L., Chasis, J. A., Delaunay, J., Mohandas, N., Anstee, D. J., and Tanner, M. J. (2003) A band 3-based macrocomplex of integral and peripheral proteins in the RBC membrane. *Blood* **101,** 4180–4188
3. Lee, J. C., and Discher, D. E. (2001) Deformation-enhanced fluctuations in the red cell skeleton with theoretical relations to elasticity, connectivity, and spectrin unfolding. *Biophys. J.* **81,** 3178–3192
4. Paramore, S., Ayton, G. S., Mirijanian, D. T., and Voth, G. A. (2006) Extending a spectrin repeat unit. I: linear force-extension response. *Biophys. J.* **90,** 92–100
5. Bennett, V., and Stenbuck, P. J. (1980) Association between ankyrin and the cytoplasmic domain of band 3 isolated from the human erythrocyte membrane. *J. Biol. Chem.* **255,** 6424–6432
6. Lux, S. E. (1979) Dissecting the red cell membrane skeleton. *Nature* **281,** 426–429
7. Bruce, L. J., Ring, S. M., Ridgwell, K., Reardon, D. M., Seymour, C. A., Van Dort, H. M., Low, P. S., and Tanner, M. J. (1999) Southeast Asian ovalocytic (SAO) erythrocytes have a cold sensitive cation leak: implications for *in vitro* studies on stored SAO red cells. *Biochim. Biophys. Acta* **1416,** 258–270
8. Michaely, P., Tomchick, D. R., Machius, M., and Anderson, R. G. (2002) Crystal structure of a 12 ANK repeat stack from human ankyrinR. *EMBO J.* **21,** 6387–6396
9. Thevenin, B. J., and Low, P. S. (1990) Kinetics and regulation of the ankyrin-band 3 interaction of the human red blood cell membrane. *J. Biol. Chem.* **265,** 16166–16172
10. Kim, S., Brandon, S., Zhou, Z., Cobb, C. E., Edwards, S. J., Moth, C. W., Parry, C. S., Smith, J. A., Lybrand, T. P., Hustedt, E. J., and Beth, A. H. (2011) Determination of structural models of the complex between the cytoplasmic domain of erythrocyte band 3 and ankyrin-R repeats 13–24. *J. Biol. Chem.* **286,** 20746–20757
11. Chang, S. H., and Low, P. S. (2003) Identification of a critical ankyrin-binding loop on the cytoplasmic domain of erythrocyte membrane band 3 by crystal structure analysis and site-directed mutagenesis. *J. Biol. Chem.* **278,** 6879–6884
12. Rank, G., Sutton, R., Marshall, V., Lundie, R. J., Caddy, J., Romeo, T., Fernandez, K., McCormack, M. P., Cooke, B. M., Foote, S. J., Crabb, B. S., Curtis, D. J., Hilton, D. J., Kile, B. T., and Jane, S. M. (2009) Novel roles for erythroid ankyrin-1 revealed through an ENU-induced null mouse mutant. *Blood* **113,** 3352–3362
13. Hughes, M. R., Anderson, N., Maltby, S., Wong, J., Berberovic, Z., Birkenmeier, C. S., Haddon, D. J., Garcha, K., Flenniken, A., Osborne, L. R., Adamson, S. L., Rossant, J., Peters, L. L., Minden, M. D., Paulson, R. F., Wang, C., Barber, D. L., McNagny, K. M., and Stanford, W. L. (2011) A novel ENU-generated truncation mutation lacking the spectrin-binding and C-terminal regulatory domains of Ank1 models severe hemolytic hereditary spherocytosis. *Exp. Hematol.* **39,** 305–320
14. Peters, L. L., Swearingen, R. A., Andersen, S. G., Gwynn, B., Lambert, A. J., Li, R., Lux, S. E., and Churchill, G. A. (2004) Identification of quantitative trait loci that modify the severity of hereditary spherocytosis in wan, a new mouse model of band-3 deficiency. *Blood* **103,** 3233–3240
15. Southgate, C. D., Chishti, A. H., Mitchell, B., Yi, S. J., and Palek, J. (1996) Targeted disruption of the murine erythroid band 3 gene results in spherocytosis and severe hemolytic anemia despite a normal membrane skeleton. *Nat. Genet.* **14,** 227–230
16. Bennett, V., and Healy, J. (2008) Organizing the fluid membrane bilayer: diseases linked to spectrin and ankyrin. *Trends Mol. Med.* **14,** 28–36
17. Lux, S. E., Tse, W. T., Menninger, J. C., John, K. M., Harris, P., Shalev, O., Chilcote, R. R., Marchesi, S. L., Watkins, P. C., and Bennett, V. (1990) Hereditary spherocytosis associated with deletion of human erythrocyte ankyrin gene on chromosome 8. *Nature* **345,** 736–739
18. van den Akker, E., Satchwell, T. J., Williamson, R. C., and Toye, A. M. (2010) Band 3 multiprotein complexes in the red cell membrane: of mice and men. *Blood Cells Mol. Dis.* **45,** 1–8
19. Peters, L., and Barker, J. (2001) Spontaneous and targeted mutations in erythrocyte membrane skeleton genes: mouse models hereditary spherocytosis, in *Hematopoiesis: A Developmental Approach* (LI, Z., ed) pp. 582–608, Oxford University Press, New York
20. Anong, W. A., Franco, T., Chu, H., Weis, T. L., Devlin, E. E., Bodine, D. M., An, X., Mohandas, N., and Low, P. S. (2009) Adducin forms a bridge between the erythrocyte membrane and its cytoskeleton and regulates membrane cohesion. *Blood* **114,** 1904–1912
21. Alloisio, N., Dalla Venezia, N., Rana, A., Andrabi, K., Texier, P., Gilsanz, F., Cartron, J. P., Delaunay, J., and Chishti, A. H. (1993) Evidence that red blood cell protein p55 may participate in the skeleton-membrane linkage that involves protein 4.1 and glycophorin C. *Blood* **82,** 1323–1327
22. Marfatia, S. M., Leu, R. A., Branton, D., and Chishti, A. H. (1995) Identification of the protein 4.1 binding interface on glycophorin C and p55, a homologue of the *Drosophila* discs large tumor suppressor protein. *J. Biol. Chem.* **270,** 715–719
23. Marfatia, S. M., Lue, R. A., Branton, D., and Chishti, A. H. (1994) *In vitro* binding studies suggest a membrane-associated complex between erythroid p55, protein 4.1, and glycophorin C. *J. Biol. Chem.* **269,** 8631–8634
24. Burton, N. M., and Bruce, L. J. (2011) Modeling the structure of the red cell membrane. *Biochem. Cell Biol.* **89,** 200–215
25. Khan, A. A., Hanada, T., Mohseni, M., Jeong, J. J., Zeng, L., Gaetani, M., Li, D., Reed, B. C., Speicher, D. W., and Chishti, A. H. (2008) Dematin and adducin provide a novel link between the spectrin cytoskeleton and human erythrocyte membrane by directly interacting with glucose transporter-1. *J. Biol. Chem.* **283,** 14600–14609
26. Low, P. S. (1986) Structure and function of the cytoplasmic domain of band 3: center of erythrocyte membrane-peripheral protein interactions. *Biochim. Biophys. Acta* **864,** 145–167
27. Mohandas, N., and Chasis, J. A. (1993) Red blood cell deformability, membrane material properties and shape: regulation by transmembrane, skeletal, and cytosolic proteins and lipids. *Semin. Hematol.* **30,** 171–192
28. Tsuji, A., Kawasaki, K., Ohnishi, S., Merkle, H., and Kusumi, A. (1988) Regulation of band 3 mobilities in erythrocyte ghost membranes by protein association and cytoskeletal meshwork. *Biochemistry* **27,** 7447–7452
29. Nigg, E. A., and Cherry, R. J. (1980) Anchorage of a band 3 population at the erythrocyte cytoplasmic membrane surface: protein rotational diffusion measurements. *Proc. Natl. Acad. Sci. U.S.A.* **77,** 4702–4706
30. Corbett, J. D., Agre, P., Palek, J., and Golan, D. E. (1994) Differential control of band 3 lateral and rotational mobility in intact red cells. *J. Clin. Invest.* **94,** 683–688
31. Blackman, S. M., Cobb, C. E., Beth, A. H., and Piston, D. W. (1996) The orientation of eosin-5-maleimide on human erythrocyte band 3 measured by fluorescence polarization microscopy. *Biophys. J.* **71,** 194–208
32. Matayoshi, E. D., and Jovin, T. M. (1991) Rotational diffusion of band 3 in erythrocyte membranes. 1. Comparison of ghosts and intact cells. *Biochemistry* **30,** 3527–3538

33. Golan, D. E., and Veatch, W. (1980) Lateral mobility of band 3 in the human erythrocyte membrane studied by fluorescence photobleaching recovery: evidence for control by cytoskeletal interactions. *Proc. Natl. Acad. Sci. U.S.A.* **77,** 2537–2541
34. Tsuji, A., and Ohnishi, S. (1986) Restriction of the lateral motion of band 3 in the erythrocyte membrane by the cytoskeletal network: dependence on spectrin association state. *Biochemistry* **25,** 6133–6139
35. Kodippili, G. C., Spector, J., Sullivan, C., Kuypers, F. A., Labotka, R., Gallagher, P. G., Ritchie, K., and Low, P. S. (2009) Imaging of the diffusion of single band 3 molecules on normal and mutant erythrocytes. *Blood* **113,** 6237–6245
36. Tomishige, M., and Kusumi, A. (1999) Compartmentalization of the erythrocyte membrane by the membrane skeleton: intercompartmental hop diffusion of band 3. *Mol. Biol. Cell* **10,** 2475–2479
37. Tomishige, M., Sako, Y., and Kusumi, A. (1998) Regulation mechanism of the lateral diffusion of band 3 in erythrocyte membranes by the membrane skeleton. *J. Cell Biol.* **142,** 989–1000
38. Mirchev, R., Lam, A., and Golan, D. E. (2011) Membrane compartmentalization in Southeast Asian ovalocytosis red blood cells. *Br. J. Haematol.* **155,** 111–121
39. Peters, L. L., Birkenmeier, C. S., and Barker, J. E. (1992) Fetal compensation of the hemolytic anemia in mice homozygous for the normoblastosis (nb) mutation. *Blood* **80,** 2122–2127
40. Gilligan, D. M., Lozovatsky, L., Gwynn, B., Brugnara, C., Mohandas, N., and Peters, L. L. (1999) Targeted disruption of the β-adducin gene (Add2) causes red blood cell spherocytosis in mice. *Proc. Natl. Acad. Sci. U.S.A.* **96,** 10717–10722
41. Robledo, R. F., Ciciotte, S. L., Gwynn, B., Sahr, K. E., Gilligan, D. M., Mohandas, N., and Peters, L. L. (2008) Targeted deletion of α-adducin results in absent β- and γ-adducin, compensated hemolytic anemia, and lethal hydrocephalus in mice. *Blood* **112,** 4298–4307
42. Robledo, R. F., Ciciotte, S. L., Gwynn, B., Sahr, K. E., Gilligan, D. M., and Peters, L. L. (2007) Targeted deletion of alpha-adducin results in absent beta-adducin, compensated hemolytic anemia, and hydrocephalus in mice. *Blood* **110,** 49A–49A
43. Peters, L. L., Birkenmeier, C. S., Bronson, R. T., White, R. A., Lux, S. E., Otto, E., Bennett, V., Higgins, A., and Barker, J. E. (1991) Purkinje cell degeneration associated with erythroid ankyrin deficiency in nb/nb mice. *Journal of Cell Biology* **114,** 1233–1241
44. Kodippili, G. C., Spector, J., Kang, G. E., Liu, H., Wickrema, A., Ritchie, K., and Low, P. S. (2010) Analysis of the kinetics of band 3 diffusion in human erythroblasts during assembly of the erythrocyte membrane skeleton. *Br. J. Haematol.* **150,** 592–600
45. Gelles, J., Schnapp, B. J., and Sheetz, M. P. (1988) Tracking kinesin-driven movements with nanometer-scale precision. *Nature* **331,** 450–453
46. Salhany, J. M. (2001) Mechanistic basis for site-site interactions in inhibitor and substrate binding to band 3 (AE1): evidence distinguishing allosteric from electrostatic effects. *Blood Cells Mol. Dis.* **27,** 901–912
47. Golan, D. E., Alecio, M. R., Veatch, W. R., and Rando, R. R. (1984) Lateral mobility of phospholipid and cholesterol in the human erythrocyte membrane: effects of protein-lipid interactions. *Biochemistry* **23,** 332–339
48. Birkenmeier, C. S., Gifford, E. J., and Barker, J. E. (2003) Normoblastosis, a murine model for ankyrin-deficient hemolytic anemia, is caused by a hypomorphic mutation in the erythroid ankyrin gene Ank1. *Hematol. J.* **4,** 445–449
49. Yi, S. J., Liu, S. C., Derick, L. H., Murray, J., Barker, J. E., Cho, M. R., Palek, J., and Golan, D. E. (1997) Red cell membranes of ankyrin-deficient nb/nb mice lack band 3 tetramers but contain normal membrane skeletons. *Biochemistry* **36,** 9596–9604
50. Bennett, V. (1979) Immunoreactive forms of human erythrocyte ankyrin are present in diverse cells and tissues. *Nature* **281,** 597–599
51. Hughes, C. A., and Bennett, V. (1995) Adducin: a physical model with implications for function in assembly of spectrin-actin complexes. *J. Biol. Chem.* **270,** 18990–18996
52. Smith, D. K., and Palek, J. (1982) Modulation of lateral mobility of band 3 in the red cell membrane by oxidative cross-linking of spectrin. *Nature* **297,** 424–425
53. Sheetz, M. P., Schindler, M., and Koppel, D. E. (1980) Lateral mobility of integral membrane proteins is increased in spherocytic erythrocytes. *Nature* **285,** 510–511
54. Mirchev, R., and Golan, D. E. (2001) Single-particle tracking and laser optical tweezers studies of the dynamics of individual protein molecules in membranes of intact human and mouse red cells. *Blood Cells Mol. Dis.* **27,** 143–147
55. Peters, L. L., Jindel, H. K., Gwynn, B., Korsgren, C., John, K. M., Lux, S. E., Mohandas, N., Cohen, C. M., Cho, M. R., Golan, D. E., and Brugnara, C. (1999) Mild spherocytosis and altered red cell ion transport in protein 4.2-null mice. *J. Clin. Invest.* **103,** 1527–1537
56. Blackman, S. M., Hustedt, E. J., Cobb, C. E., and Beth, A. H. (2001) Flexibility of the cytoplasmic domain of the anion exchange protein, band 3, in human erythrocytes. *Biophys. J.* **81,** 3363–3376
57. Nigg, E. A., and Cherry, R. J. (1979) Influence of temperature and cholesterol on the rotational diffusion of band 3 in the human erythrocyte membrane. *Biochemistry* **18,** 3457–3465
58. Satchwell, T. J., Shoemark, D. K., Sessions, R. B., and Toye, A. M. (2009) Protein 4.2: a complex linker. *Blood Cells Mol. Dis.* **42,** 201–210
59. Salomao, M., Zhang, X., Yang, Y., Lee, S., Hartwig, J. H., Chasis, J. A., Mohandas, N., and An, X. (2008) Protein 4.1R-dependent multiprotein complex: new insights into the structural organization of the red blood cell membrane. *Proc. Natl. Acad. Sci. U.S.A.* **105,** 8026–8031
60. Campanella, M. E., Chu, H., and Low, P. S. (2005) Assembly and regulation of a glycolytic enzyme complex on the human erythrocyte membrane. *Proc. Natl. Acad. Sci. U.S.A.* **102,** 2402–2407
61. Shultz, L. D., Rajan, T. V., and Greiner, D. L. (1997) Severe defects in immunity and hematopoiesis caused by SHP-1 protein-tyrosine phosphatase deficiency. *Trends Biotechnol.* **15,** 302–307